scientific reports



OPEN

Research and application of 3D attribute fusion technology based on lithology probability analysis

Shanyi Zhang^{1,2⊠}, Xueying Li¹, Jinyu Lan², Dejian Zhang², Lin Cong¹ & Yaning Shi¹

To address the challenges of seismic attribute selection and the low accuracy of characterizing single-phase river channels with a single seismic attribute, a 3D seismic attribute fusion technology based on lithology probability curve analysis has been developed. This method uses lithology probability curve analysis to optimally select amplitude attributes that highlight the distribution characteristics of sedimentary sand bodies and coherence attributes that emphasize variations in sand body boundaries. These attributes are then fused to form a new attribute volume, effectively solving the issues of seismic attribute selection and the low precision of single attributes in characterizing river channels. The approach enables precise identification of single-phase river channels and improves the sand body prediction accuracy in the study area by 20.2% points. The results have been applied to guide the optimization of 112 well interventions, resulting in an accumulated oil increase of 10,861 tons. This demonstrates favorable outcomes and provides a geological foundation for the accurate exploitation of residual oil in high-water-cut late-stage reservoirs.

Keywords Attribute fusion, Amplitude attributes, Coherence attributes, Lithology probability analysis, River channel sand bodies

After years of technical development, seismic reservoir prediction methods have become relatively mature. Due to the different sensitivities of various seismic attributes to different geological phenomena, these methods have been widely applied in oilfield production to predict subsurface geological conditions, with favorable results^{1–16}. However, there are still issues related to seismic attribute selection and the interpretation of single seismic attributes, such as ambiguity and multiple solutions, which require further improvement.

Currently, selecting a single seismic attribute is challenging. There are dozens of amplitude-type seismic attributes that reflect the changes in sandstone and mudstone, and selecting the best attribute from these to identify subsurface sandstone and mudstone reservoirs is difficult. Traditional methods typically involve projecting the sandstone and mudstone information from well data onto various seismic attribute slices for visual comparison 17-20, or comparing seismic attributes with lithology isovalue maps from well data 21-32. The seismic attributes that can distinguish sandstone from mudstone are qualitatively identified, and then each attribute is analyzed to determine its correspondence with well data. The attribute with the highest match rate is selected. This process is not only tedious and labor-intensive but also subject to human bias, leading to inconsistencies in the seismic attribute selection results from different technicians.

To address the challenges of identifying reservoir lithology using a single seismic attribute, many researchers have explored multi-attribute fusion techniques. These methods combine the advantages of different attributes to resolve the ambiguities in identifying lithology with a single attribute. Multi-attribute fusion technology can integrate the strengths of various attributes, providing more reliable information for reservoir prediction and improving prediction accuracy, which is essential for precise residual oil exploitation in high-water-cut late-stage reservoirs^{33,34}. Current seismic multi-attribute fusion methods include clustering analysis based on mathematical methods³⁵, linear regression³⁶, iterative methods³⁷, and other fusion techniques; color-space-based RGBA fusion³⁸, RGB rendering³⁹, and RGB-IHS transformation⁴⁰; as well as neural network-based fusion methods⁴¹. However, excessive human intervention in the original seismic data during the fusion process may introduce artifacts, leading to inaccurate interpretation results.

Given the variety of seismic attribute fusion methods and the lack of clear criteria for their applicability and quantitative assessment, effective and standardized fusion methods have not yet been established 42,43.

¹State Key Laboratory of Continental Shale Oil, Northeast Petroleum University, Daqing 163318, Heilongjiang, China. ²China Petroleum Daqing Oilfield Company Limited, Daqing 163513, Heilongjiang, China. [⊠]email: zsy0537@sina.com

In the Daqing Changyuan area, the primary geological features are river-delta plains and inner delta front environments, characterized by thin sand bodies and rapid lateral facies changes. These features make it difficult to rely solely on well data and single seismic attributes for reservoir prediction⁴⁴, which in turn affects oilfield development. Particularly in the late-stage high-water-cut production phase, the focus of fine geological studies is to accurately determine the boundaries and connectivity of river channels⁴⁵. Therefore, this paper proposes a 3D attribute fusion technique based on lithology probability analysis. This method can quantitatively select the most effective seismic attributes from a wide range of seismic data and, during fusion, retain as much of the geological information reflected by the seismic data as possible, minimizing human interference and improving the accuracy and reliability of the geological interpretation. The technique provides technical support for accurate identification of single-phase river channel boundaries and enhances residual oil recovery in the late high-water-cut stage.

Research methods

Before performing seismic attribute fusion, it is first necessary to optimize individual seismic attributes. The specific steps are as follows: First, by analyzing the correlation between each seismic attribute and reservoir lithology, seismic attributes that are most sensitive to the different geological features in the study area are selected. Next, different attributes are fused, but only the portions above the sandstone threshold are retained, while mudstone parts below the threshold are filtered out. Finally, these seismic attributes, which have different sensitivities, are interpreted to describe the development characteristics of the underground reservoir.

Seismic attribute lithology probability curve analysis method

This study investigates seismic attribute lithology and microfacies encounter probability curve analysis techniques, and combines them with the correlation coefficient method to form a fast and accurate seismic attribute selection process. The first step is to extract dozens of seismic attributes for a particular layer. Then, through Pearson's correlation coefficient analysis, the 3–5 seismic attributes with the highest correlation are initially selected. Next, the threshold values for sandstone and mudstone for these selected attributes are calculated, and probability curves are plotted to directly and quantitatively assess whether these attributes can identify sandstone and mudstone. Finally, the seismic attributes that show strong ability to identify sandstone and mudstone are selected.

(1) Pearson's correlation coefficient analysis method

The seismic attributes extracted for a particular layer are analyzed by comparing the attribute values at well locations with the thickness of the sandstone at those points. Pearson's correlation coefficient is calculated, and the top 3–5 seismic attributes with the highest correlation are selected. In the study area, the correlation between seismic attributes and sandstone thickness is typically below 0.4. It is observed that when the correlation between seismic attributes and sandstone thickness is greater than 0.3, the attribute can identify river-channel sands to some extent. However, when the correlation is below 0.3, the attribute has little utility for identifying river-channel sands. Therefore, seismic attributes with a Pearson correlation coefficient greater than 0.3 with sandstone thickness should be selected initially, and further refinement can be carried out.

(2) Lithology or sedimentary microfacies probability analysis method

Using the initial selection from the Pearson's correlation coefficient analysis, a more refined selection is made using lithology or microfacies probability analysis, based on seismic attribute data and well data. This method allows for a more intuitive representation of which attributes are most effective in identifying sandstone and which are better for identifying mudstone, making the attribute selection process more accurate and convenient. This method can intuitively characterize which attribute has a strong ability to identify sandstone and which attribute is more effective for identifying mudstone, thereby facilitating a more convenient and accurate selection of seismic attributes. It addresses the previous approach, which involved comparing various seismic attributes with sandstone isopach maps based on well data for a specific layer, qualitatively determining the attributes that distinguish sandstone from mudstone, and then analyzing the consistency of these attributes at well points. This process required statistical analysis of well point consistency rates to determine whether the seismic attributes could effectively identify sandstone and mudstone. The traditional method was highly complex, involved significant workload, and was prone to substantial human influence.

First, the relationship between seismic attribute values at well locations and sandstone thickness or sedimentary microfacies is analyzed. A scatter plot of seismic attribute values versus sandstone thickness is drawn to determine the correlation between the seismic attributes and both sandstone and mudstone.

Next, the lithology and microfacies probabilities for each seismic attribute value are calculated. For example, taking the SIII9 amplitude attribute as an example in the Fig. 1, since amplitude is negatively correlated with sandstone thickness, when a threshold value X is used, the interval $[X_{\min}, X]$ corresponds to the sandstone zone, where sandstone thickness is greater than 1 m, but the threshold can be adjusted as needed, and the interval $(X, X_{\max}]$ corresponds to the mudstone zone.

 $X_{
m max}$] corresponds to the mudstone zone. The sandstone probability at X is defined as the ratio of the number of wells in the sandstone zone with seismic attribute values between $X_{
m min}$ and X to the total number of wells in the sandstone zone. Similarly, the mudstone probability is defined as the ratio of the number of wells in the mudstone zone with seismic attribute values between X and $X_{
m max}$ to the total number of wells in the mudstone zone. The meaning of the sandstone probability in the sandstone zone is that if the attribute values between $X_{
m min}$ and X are considered as representing the sandstone zone, then the probability of encountering sandstone in this zone is S_X , while the probability of encountering mudstone in the mudstone zone with attribute values between X and $X_{
m max}$ is N_X . At this point, the

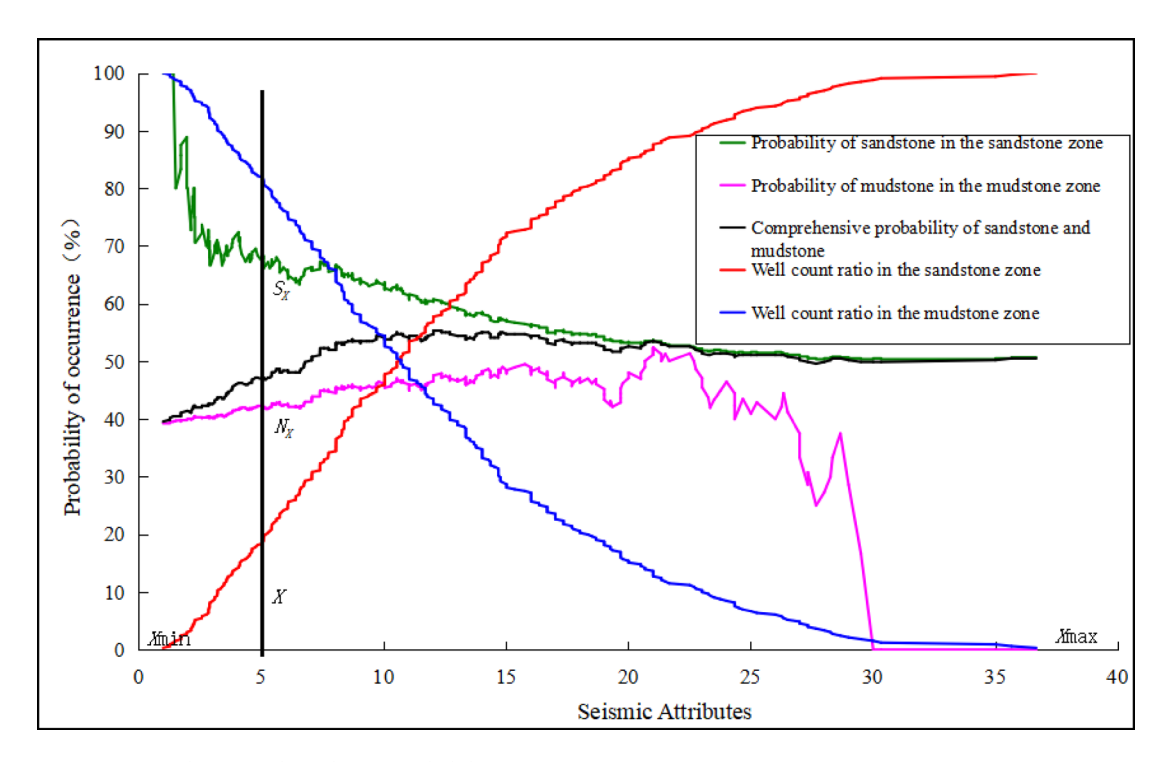


Fig. 1. Sandstone and Mudstone Probability Curves.

ratio of wells in the sandstone zone is the ratio of the total number of wells in the sandstone zone to the total number of wells used in the probability calculation; similarly, the ratio of wells in the mudstone zone is the ratio of the total number of wells in the mudstone zone to the total number of wells used in the probability calculation.

Finally, when all seismic attribute values are used as threshold values, probability curves for sandstone, mudstone, combined sandstone-mudstone, and the proportion of wells in the sandstone and mudstone zones are plotted. The resulting sandstone and mudstone probability curves intuitively show how the seismic attribute value at a given threshold X divides the seismic data into two regions: the sandstone zone and the mudstone zone. These curves also represent the predictive probability of lithology and the area proportions of the sandstone and mudstone zones, allowing for a quick and accurate judgment of the seismic attribute's ability to predict sandstone and mudstone.

The advantage of using probability curve analysis for seismic attribute selection is that it automatically calculates the probabilities of encountering sandstone or mudstone in different attribute ranges and the probabilities of encountering specific microfacies in river-channel, river-interfluve or termination zones. The method provides an intuitive, quantitative, and precise representation of attribute characteristics, is not influenced by human bias, and improves the accuracy and convenience of interpretation. This greatly enhances the efficiency and quality of seismic attribute selection.

Moreover, based on the actual requirements and prediction accuracy for different reservoirs, suitable threshold values can be read directly from the lithology probability curves for reservoir prediction. Multiple threshold values can be set to define regions with different prediction accuracies, thereby guiding more accurate subsurface reservoir prediction. For example, if the predicted accuracy for sandstone thickness in a target layer based on well data is 70%, then the attribute ranges with a probability greater than 70% can be used for reservoir prediction. Additionally, multiple thresholds, such as 70%, 80%, or 90%, can be set, and the reservoir prediction can be adjusted according to the prediction capabilities of each interval, thus improving the overall prediction accuracy as much as possible.

Coherence attribute calculation methods

The lithology probability-based method is effective in distinguishing between sandstone and mudstone; however, since the transition between these two is gradual, accurately delineating sandstone boundaries can be challenging. To address this, seismic coherence attributes can be preferentially used to identify the boundaries of sandstone bodies. Coherence attributes are particularly effective in capturing boundary delineation. There are several coherence algorithms, each with varying strengths in identifying different subsurface geological bodies.

Currently, coherence algorithms primarily include the cross-correlation algorithm, similarity coefficient algorithm, intrinsic structural analysis algorithm, and multi-operator coherence algorithm based on sub-body attributes. Each method has its own strengths and limitations, making them suitable for different geological conditions

Cross-correlation algorithm: This algorithm calculates the correlation coefficient between the main survey line and the connecting survey lines and then synthesizes the results. It is computationally efficient and easy to implement, but it has limited noise resistance.

Similarity coefficient algorithm: This algorithm calculates the coherence between multiple seismic traces and is highly stable and noise-resistant. Additionally, it allows for adjustable window lengths. However, it does not account for the effects of layer dip, which can affect its applicability.

Intrinsic structural analysis algorithm: This method calculates coherence directly from the 3D seismic data, without requiring layer constraints, and offers higher resolution. However, it does not consider layer dip and azimuth, which can reduce its accuracy under certain geological conditions.

Multi-operator coherence algorithm based on sub-body attributes: This algorithm uses multiple coherence operators applied to sub-body attributes, enabling multi-information detection. It offers higher resolution and is particularly advantageous for identifying complex geological bodies, such as narrow river channel sand bodies.

Coherence analysis parameters primarily include window size, number of seismic traces, dip angle, spatial arrangement of seismic traces, and the orientation of the seismic data. The selection of these parameters directly impacts the calculation speed and the effectiveness of predicting river channel sand body boundaries.

Number of seismic traces: Increasing the number of seismic traces reduces noise and improves the signal-tonoise ratio. However, using too many traces can reduce the lateral resolution of the coherence attribute.

Coherence window size: If the window is too small, the resulting coherence data will primarily reflect noise. Conversely, a larger window reduces noise but lowers resolution, causing geological features to become blurred.

Optimization of window placement: By adjusting the coherence window within the search range, the central seismic trace can be optimally aligned with adjacent traces. This helps to select the best parameter values and mitigates the impact of layer dip on the seismic coherence results.

Through experimentation with various parameters, including seismic trace count, dip angle, and window size, we identified the key parameters that influence the results of coherence analysis. Using 3D seismic data in the time domain, we calculated the coherence parameters for the study area and summarized the prediction results for different parameter combinations (Table 1).

When selecting $\hat{4}$ traces with a window of +/-1 ms, the seismic data becomes too noisy, making it impossible to identify the river channel (Fig. 2a). With 1 trace and a window of +/-6 ms, the seismic information is overly smoothed, preventing clear identification of the river channel (Fig. 2b). However, using 2 traces with a window of +/-3 ms yields the best results (Fig. 2c). Based on this analysis, the optimal choice is 2 traces with a window of +/-3 ms, as it provides the clearest and most accurate identification of the river channel.

The figures are generated by using the version 6 of Generic Mapping Tools https://www.generic-mapping-tools.org/.

Three -dimensional seismic attribute fusion

In response to the development characteristics of different reservoirs, a three -dimensional seismic attribute meeting fusion and transparency control fusion method have been developed, which can well realize the fine identification of different sand bodies of underground reservoirs.

(1) Three -dimensional seismic attributes fusion technology

Give a fixed value, add this fixed value to the amplitude body to form a new fusion. This fusion method has changed the value of some fusion boundaries and strengthened some weak boundaries.

Complete the advantages of conventional strata slices on the overall display trend of the reservoir of the river sand body and the compatible body's advantages in the boundary detection of the river sand body border, and the fusion body slices further improve the accuracy of the reservoir forecasting on the basis of the formation of the strata; Value is equivalent to enhancing part of the phase dry value. Under certain conditions, it can enhance the clarity of the boundary of a single river sand body, and it is more suitable for the identification of large composite river tract sand bodies and internal non -average boundaries. Add this fixed value to the amplitude body to form a new fusion. This fusion method has changed the value of some fusion boundaries. It has strengthened some weak boundaries. Under certain conditions, it can enhance the clearness of a single river sand border boundary. Degree (Fig. 3) can realize the identification of a single sand body inside the large composite river.

For example, within the elliptical area marked in the figure, the amplitude attribute fails to clearly delineate the channel sand bodies(Fig. 4a), whereas Three-dimensional seismic attributes fusion effectively characterizes the channel sand bodies, with the channel boundaries being more distinctly defined(Fig. 4b).

Option	Parameter	River channel boundary detection	Noise attenuation	Computation speed	
	2	Best	-	Fast	
Number of Seismic Traces	4	Better	-	Medium	
	8	Good	-	Slow	
Dip Angle	0°	Poor	-	Fast	
	10°	Good	-	Slow	
	20°	Poor	-	Very Slow	
Time Window Size	1 ms	Average	Average	Faster	
	3 ms	Good	Good	Fast	
	6 ms	Average	Average	Slow	
	9 ms	Average	Average	Very Slow	

Table 1. Optimal parameters for identifying river channel boundaries in the study area.

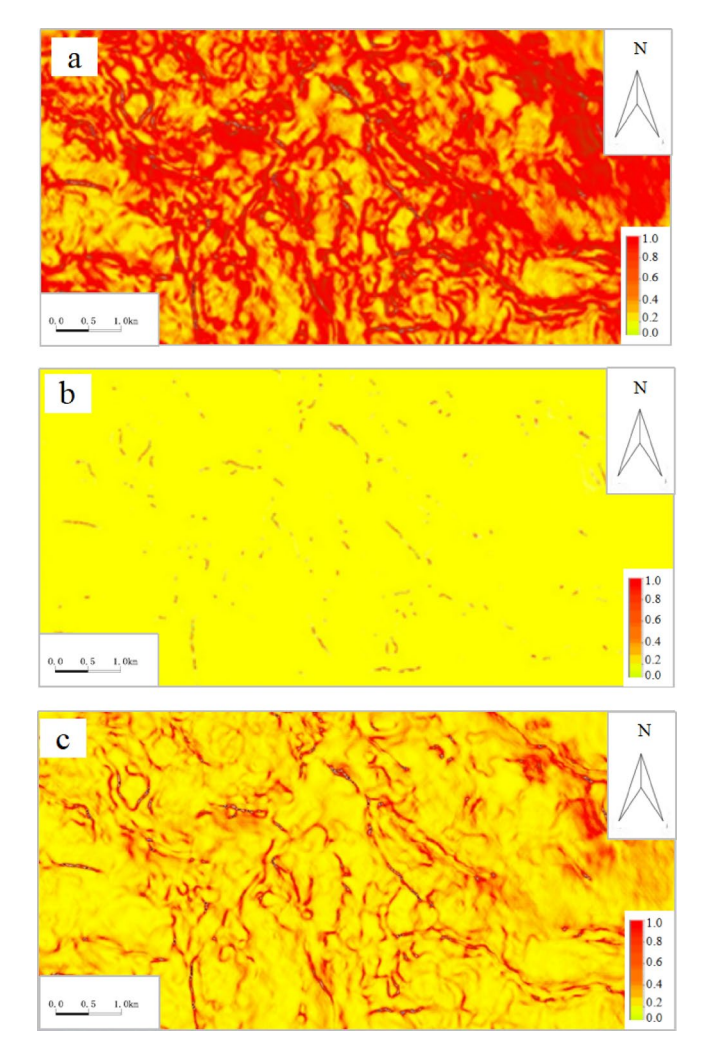


Fig. 2. Coherence Body Slices. (a) 4 traces, with a time window of ± 1 ms. (b) 1 trace, with a time window of ± 6 ms. (c) 2 traces, with a time window of ± 3 ms.

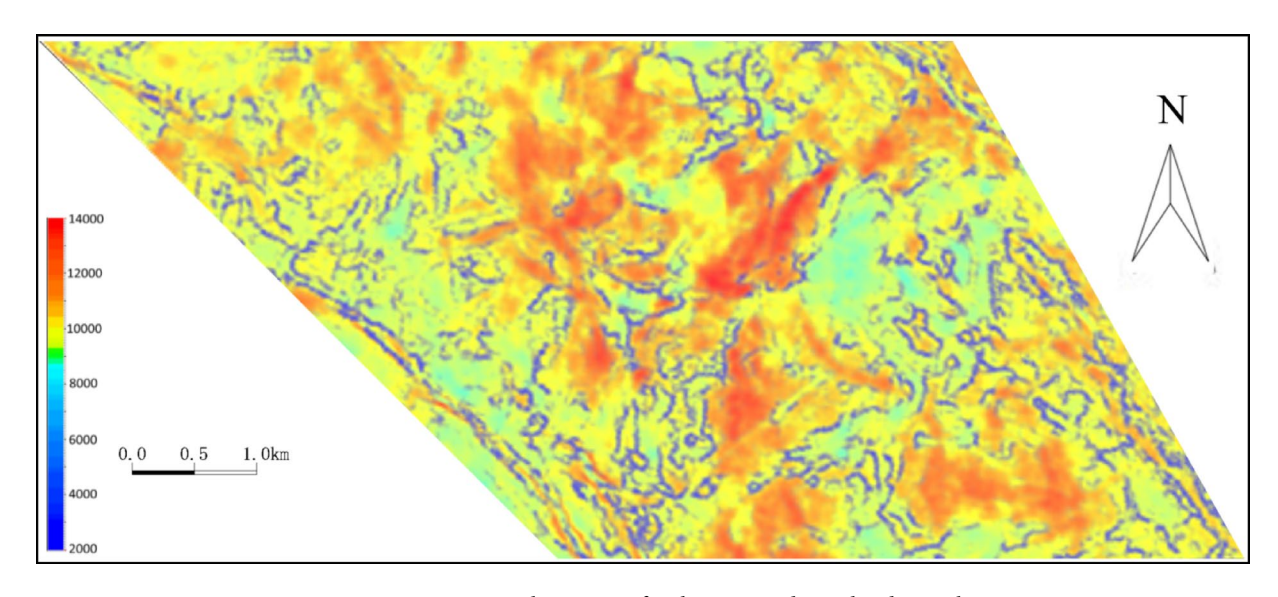


Fig. 3. 3D Intersection Fusion Attribute Map of Coherence and Amplitude Attributes.

Fig. 4. Comparison of Amplitude Attribute and 3D Seismic Attribute Fusion Attribute. (**a**) Amplitude Attribute. (**b**) Three -dimensional seismic attributes fusion Attribute.

(2) Filtering fusion technology

This technique uses amplitude attributes as the base and filters out portions of the attributes with good coherence, then overlays the filtered attribute volumes to create a new fused attribute volume. The key feature of this method is that it does not alter the coherence values themselves; instead, it performs a filtering operation on the portions with strong coherence. By identifying the boundaries of high- and low-coherence regions, this method enables the precise delineation of single-phase river channel boundaries, thus providing insights into the connectivity of sand bodies.

While individual amplitude attributes are effective at describing sand bodies, they are less effective at defining river channel boundaries (Fig. 5a). Coherence attributes, on the other hand, do a better job of capturing river channel boundaries, but they fail to depict the distribution characteristics of the sand bodies (Fig. 5b). However, when these two attributes are fused, the boundaries of the sand bodies are clearly outlined, and the variations in sand body distribution are more prominently highlighted (Fig. 5c).

This filtering fusion technology can identify subtle changes in seismic data within complex geological settings while preserving the maximum amount of geological information reflected by the seismic data. It also reduces the influence of human intervention present in other fusion methods, ensuring that the geological phenomena observed from the seismic data are more accurate and reliable. This technique supports the precise identification of river channel boundaries for single-phase surveys and provides technical assistance in optimizing the recovery of remaining oil in highly water-flooded reservoirs.

Results and discussion

The study area is located in the northern part of the Daqing Placanticline, covering an area of 9.04 km², with a well density of 275 wells/km² and a total of 2,490 wells. The target layer is the Saertu oil layer, characterized by the development of channel sand bodies that are small, scattered, and thin (Fig. 6), resulting in weak seismic reflections, which pose challenges for sand body identification. Drilling data indicate that the sand-to-mud ratio in the study area ranges between 14% and 33%. Due to the low precision in channel description and the difficulty in potential exploitation, minimizing human intervention and accurately identifying sand body connectivity are crucial. Leveraging the dense well pattern in this area, amplitude and coherence attributes were optimized, and a 3D attribute fusion method was employed to precisely delineate the boundaries of channel sand bodies in the study area.

Coherence attribute parameter optimization and amplitude attribute threshold determination

Using Pearson correlation analysis and lithology or depositional facies probability analysis methods, the probabilities of sandstone, mudstone, river channel, and termination facies were determined for the study area. Taking the SIII9 amplitude attribute as an example, the probability of sandstone development between X_{min} and X exceeds 63%. As the X value decreases, the probability increases, with areas showing probabilities greater than 80%, indicating a strong prediction ability for sandstone. In contrast, the probability of mudstone development between X and X_{max} is less than 50%, indicating a weak predictive ability for mudstone (Fig. 7). Therefore, it was concluded that the SIII9 amplitude attribute has a strong correlation with sandstone. The probability curves for river channel sand H_X and termination facies J_X are similar to the sandstone and mudstone probability curves (Fig. 7). These curves provide an intuitive representation of the seismic attributes' ability to predict river channel sands and termination facies.

The effectiveness of coherence attribute processing is primarily influenced by two key parameters: spatial aperture and time aperture. A larger spatial aperture improves the signal-to-noise ratio, but excessive spatial aperture can reduce the lateral resolution of the coherence body. Similarly, smaller time apertures tend to in-

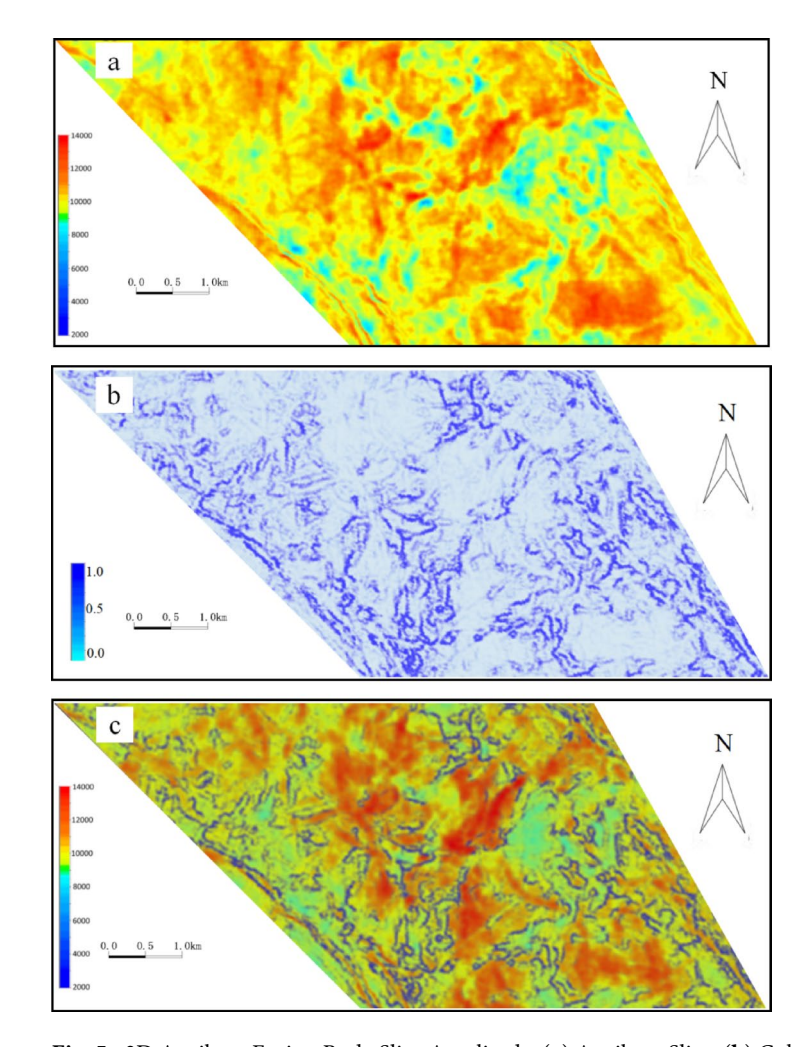


Fig. 5. 3D Attribute Fusion Body Slice Amplitude: (a) Attribute Slice, (b) Coherence Attribute Slice, (c) 3D Attribute Fusion Body. This picture is produced using PETREL2018 Software.

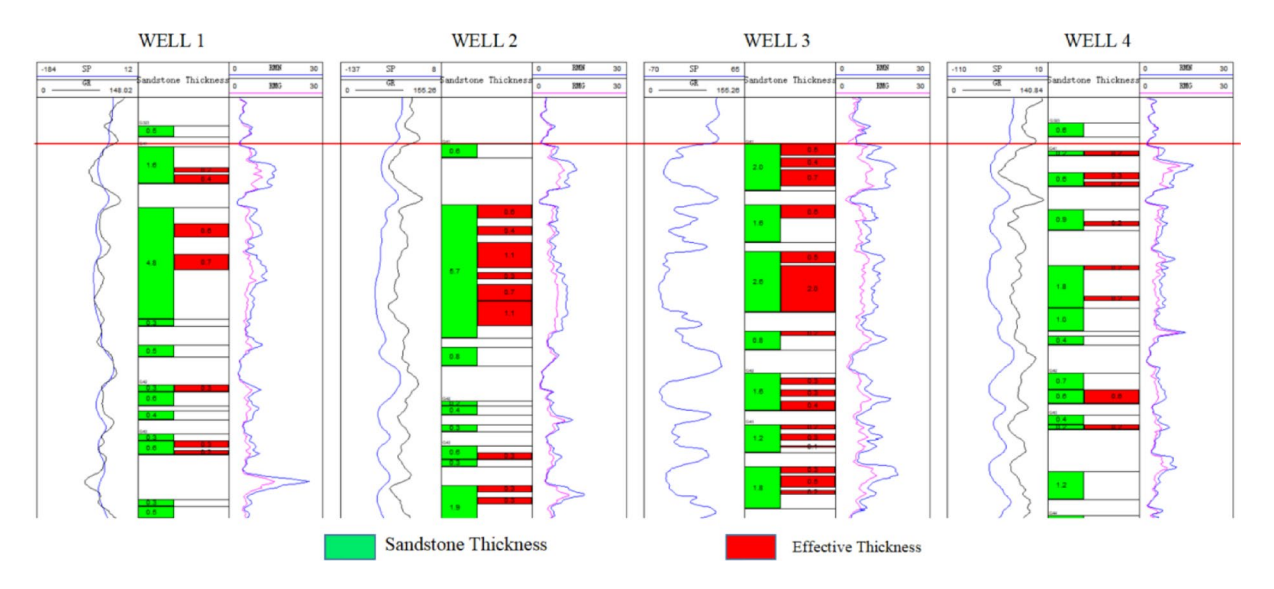


Fig. 6. Well Correlation Profile of the Study Area.

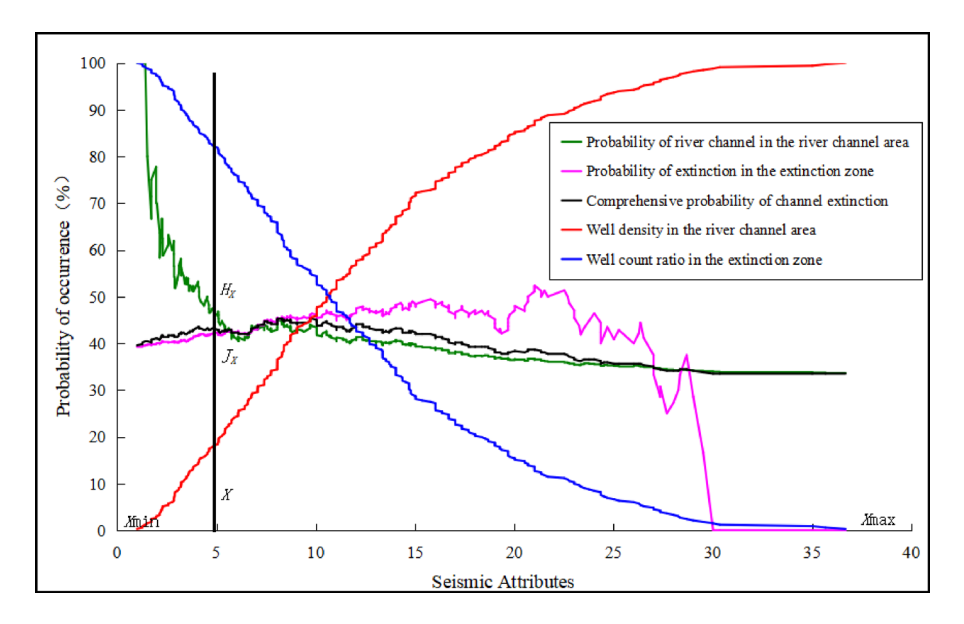


Fig. 7. River Channel and Pinch-Out Facies Probability Curve.

troduce noise, while excessively large time apertures may blur geological features. Since waveform similarity is calculated along the dip plane, selecting an appropriate dip angle is crucial for accurate coherence attribute computation. Through optimization of different time and spatial apertures and dip angles in the study area, it was found that a spatial aperture of 1, a time aperture of $\pm 1/2$ ms, and a dip angle of ± 4 ° provided the clearest reflection of river channel boundaries, with good continuity of sand bodies. These parameters meet the requirements for fine-scale prediction of sand bodies in the study area.

Coherence attribute parameter selection

The quality of coherence data processing is mainly influenced by two parameters: spatial aperture and time aperture. While larger spatial apertures improve the signal-to-noise ratio, excessively large apertures reduce the lateral resolution of the coherence body. Analysis of seismic slices from the study area's SIII9 small layer, with varying aperture sizes, showed that when the number of seismic traces was set to 1, the coherence body slice provided a clearer reflection of sand body boundaries. Smaller time apertures introduced noise, while too large a time window caused geological features to become blurred. For the SIII9 small layer in the study area, the optimal time window was found to be ± 1 0 ms, providing the clearest reflection of river channel boundaries. This method and parameter set are well-suited for fine-scale prediction of sand bodies in the area.

Three-Dimensional attribute fusion

By filtering out coherence values greater than 0.8 in SIII9 and integrating them with the amplitude attribute, the newly fused attribute effectively combines the strengths of both the amplitude attribute, which highlights the overall distribution trend of channel sand reservoirs, and the coherence attribute, which excels in detecting the boundaries of channel sand bodies. The fusion attribute slices significantly enhance the accuracy of reservoir prediction compared to traditional stratigraphic slices (Fig. 8). The results demonstrate that the channel predictions are more distinct and precise, yielding highly satisfactory outcomes.

Identification of internal boundaries in single river channel sands

In the 421-S325 well area, within a 290 m by 300 m region, the fusion technique detected several boundaries approximately 20 m in width. If these boundaries are confirmed, they could significantly impact the connectivity between the sand bodies, directly influencing the strategies for enhancing oil recovery from remaining reserves. To validate these boundaries more effectively, the area was divided into five zones: A, B, C, D, and E (Fig. 9).

Drilling data validation

Logging curve characteristics indicate different hydrodynamic environments for sandbody formation By analyzing the logging curves in Areas A, B, C, D, and E, the following conclusions were drawn regarding the hydrodynamic environments that influenced the formation of the sandbodies (Table 2):

Area A: The hydrodynamic energy of the sandbody shows a process of strong energy gradually weakening, with a decreasing supply of sediment.

Area B: The hydrodynamic energy of the sandbody increases from weak to strong, with a gradual increase in sediment supply.

Area C: The hydrodynamic energy is relatively stable, with little change in the sediment supply rate and amount.

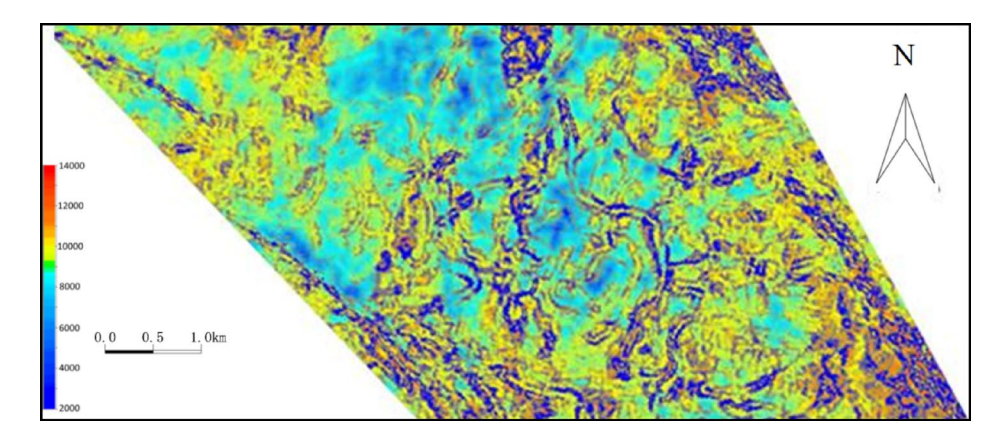


Fig. 8. Filtered Fusion Attribute Map of Coherence and Amplitude Attributes.

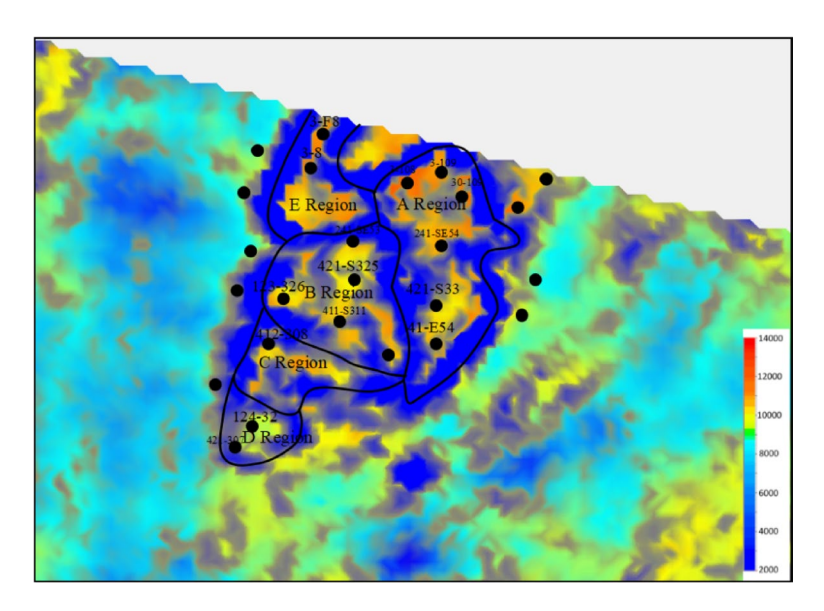


Fig. 9. Coherence and Amplitude Attribute Filtering Fusion Map.

Area D: The hydrodynamic energy weakens uniformly, or the sediment supply rate and amount decrease uniformly.

Area E: The hydrodynamic energy increases from weak to strong, or the sediment supply rate and amount increase.

Through hydrodynamic analysis, it was determined that the hydrodynamic conditions for sandbody formation in Areas A, B, C, D, and E differ. This suggests that these sandbodies were formed at different times within the same depositional period, confirming the existence of boundaries between the sandbodies.

Verifying the existence of boundaries under different water flooding conditions

The water flooding levels in the study area show distinct zonal patterns:

Zone A has high water flooding;

Zone B has moderate water flooding;

Zone C has low water flooding;

Zone D has moderate to low water flooding;

Zone E has low water flooding.

These zonal variations in water flooding are clearly defined. For instance, in adjacent wells, 123–326 in Zone B shows moderate flooding, while 412-308 in Zone C displays low flooding. Similarly, 421-S325 in Zone B experiences moderate flooding, while 421-S33 in Zone A exhibits high flooding. This suggests that the boundaries detected by the fusion technique between wells 123–326 and 412 – 308, as well as between wells 421-S325 and 421-S33, are likely to be real (Table 3).

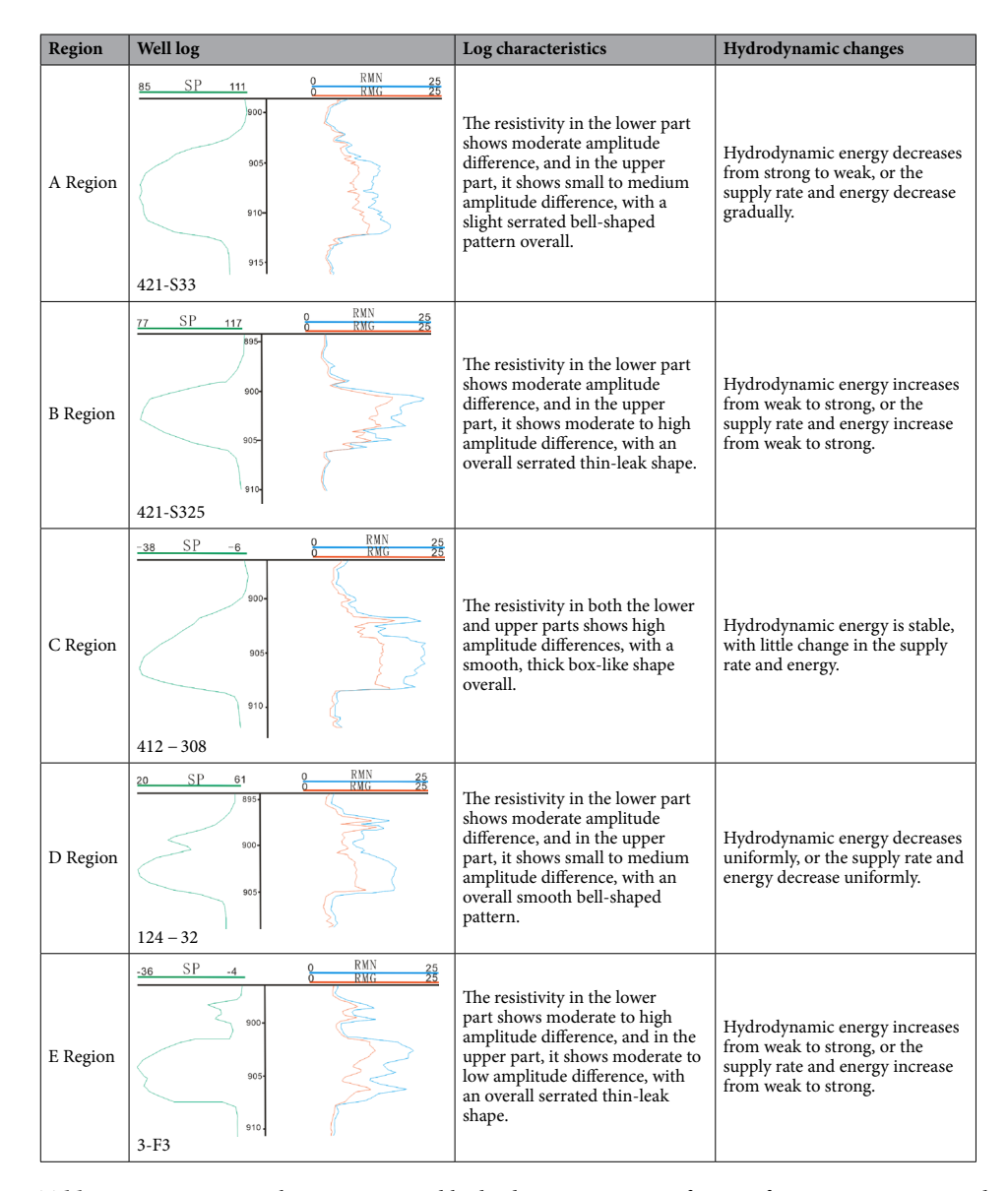


Table 2. Logging curve characteristics and hydrodynamic variation features for areas A, B, C, D, and E.

Boundary morphology exhibits abandoned river channel characteristics

The seismic data reveal boundary shapes that are S-shaped or semi-elliptical, with widths ranging from 20 to 30 m, which are typical of abandoned river channels. Modern sedimentary records show that abandoned river channels of this width are common. This strongly supports the interpretation that the boundaries identified by the fusion method correspond to abandoned river features.

Development dynamics indicate lack of connectivity between oil and water wells

In the study area, wells 241-SE54, 241-S325, and 241-SE25 all intersect sand bodies at the target layer. A tracer test was conducted at well 241-SE54 on September 30, 2014, by injecting a tracer into the well. However, no tracer was detected in either well 241-S325 or well 241-SE25, confirming that these wells are not connected. This provides further validation that the boundary identified by the fusion technique is indeed a real and significant feature.

Multi-Attribute Fusion Technology: A New Approach for Predicting Secondary and Single River Channels. The multi-attribute fusion technique presents a novel approach for predicting secondary and single river channels within complex fluvial systems. It effectively leverages the strengths of various seismic attributes, thereby enhancing the overall accuracy of reservoir predictions. In practice, different fusion methods can be applied based on local geological conditions, allowing for a more precise characterization of subsurface features and reducing the uncertainty typically associated with using a single attribute for seismic reservoir prediction.

Sandbody region	Well name	Water flooding level
A Region	3-108	High Water Flooding
A Region	3-109	High Water Flooding
A Region	30-109	High Water Flooding
A Region	241-SE54	High Water Flooding
A Region	421-S33	High Water Flooding
A Region	41-E54	High Water Flooding
B Region	421-S325	Medium Water Flooding
B Region	411-S311	Medium Water Flooding
B Region	123-326	Medium Water Flooding
B Region	241-SE53	Medium Water Flooding
C Region	412 – 308	Low Water Flooding
D Region	124 – 32	Low Water Flooding
D Region	421 – 307	Medium-Low Water Flooding
E Region	3-F8	Low Water Flooding
E Region	3-8	Low Water Flooding

Table 3. Water flooding levels of wells in different sandbody regions.

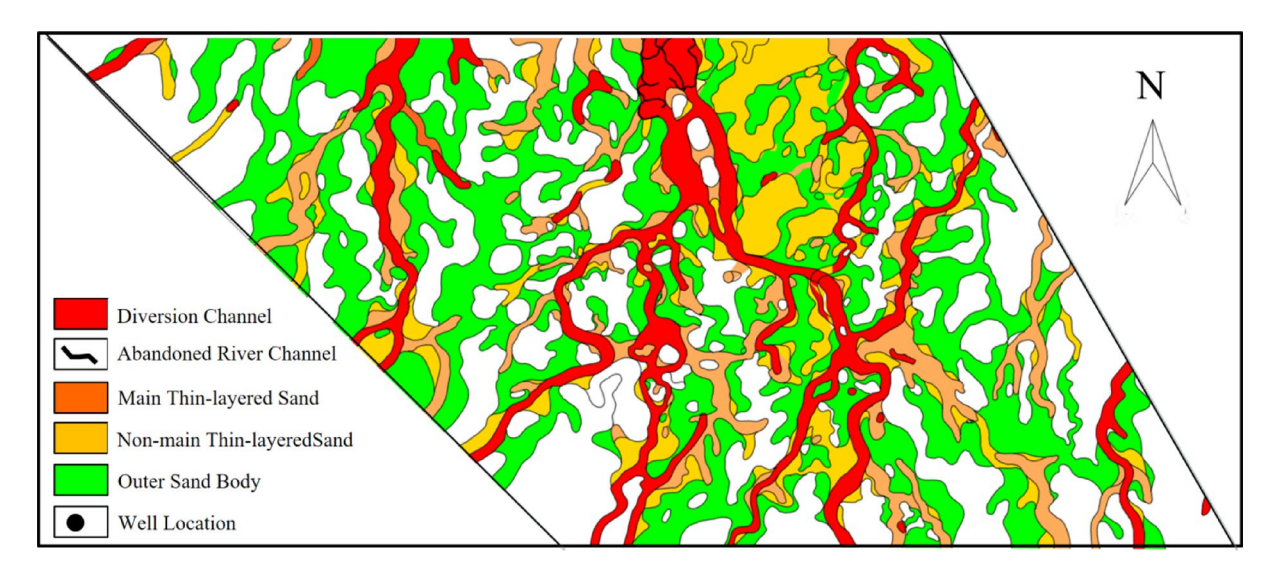


Fig. 10. Fine description of sedimentary microfacies through well-seismic integration. This figure was drawn using GPTmap, version 2017. https://www.GPTmap.com/cn/.

Fine description of typical sand bodies

The accuracy and feasibility of the fusion-based approach have been successfully validated. Using fusion technology to characterize the SIII9 layer's single river channel improved the accuracy of channel prediction from 73.6 to 93.8% by using well data alone, an increase of 20.2% points.

For example, in the SIII9 sand body (Fig. 10), the application of the fusion technique resulted in significant changes to the river channel morphology. The river flow path was not static, but fluctuated over multiple stages, ultimately forming the present-day dendritic delta system. During this process, the lake area experienced large-scale water recession and a lowering of the erosional base level, with fluvial deposition playing a dominant role. The sand body developed variable-width, ribbon-like thick sand bodies in the delta plain facies, and as it crossed the shoreline into the delta front, narrower, medium-thick sand bodies formed, oriented roughly parallel to the river flow direction. Additionally, thin, sheet-like sand bodies were deposited in the region.

The river channels in this system include both submerged and abandoned channels. The submerged channels have a minimum width of 80 m, a maximum width of 290 m, and an average width of 136 m. The thickness ranges from 1.4 m to 3.8 m, with an average thickness of 2.3 m. The channel morphology is typically ribbon-or dendritic-shaped in plan view, with a vertical sequence that becomes finer upwards. Sedimentologically, these channels exhibit medium-scale cross-bedding at the base, with significant erosion at the bottom and a gradational or sharp change at the top.

Non-channel deposits include primary sheet sand, non-primary sheet sand, and external sand bodies. The primary sheet sands are potato-shaped or dendritic in planform and exhibit sand-mud interlayers with small-

	Initial effect			Current effect			
Well number	Produced liquid (t)	Produced oil (t)	Water cut (%)	Produced liquid (t)	Produced oil (t)	Water cut (%)	Cumulative oil production (t)
3–109	79.3	5.1	93.6	36.8	5.9	84.0	581
421-S33	35.1	2.4	93.1	29.9	1.8	93.9	323
412 – 308	21.0	4.3	79.5	10.9	2.2	80.0	420
421 – 307	26.2	8.6	67.2	16.1	5.0	69.0	682
421-S325	19.1	3.8	80.0	18.1	1.0	94.3	520

Table 4. River channel sand body potential extraction effect.

scale cross-bedding and wave-like bedding, showing gradual or abrupt transitions at the top and bottom. Non-primary sheet sands have similar planform geometries but with smaller-scale cross-bedding and gradational transitions at both the top and bottom. External sand bodies are laterally continuous, with sand-mud interlayers and wave-like or small-scale cross-bedding, displaying gradual transitions at both the top and bottom.

Application effectiveness

The new research findings indicate that the planar heterogeneity of distributary river channels in the study area is strong. In many locations, the connectivity relationships evolved from a single type to three different types, leading to the formation of abandoned river channels that obscure residual oil. Additionally, the well spacing and well network could not effectively capture the distribution of residual oil. Using this new method for fine description of sedimentary facies has significantly improved the understanding of these features.

The sedimentary facies maps generated through this technique guided the adjustment of 112 wells in the study area, resulting in a total increase of 10,861 tons of oil. Among these adjustments, 5 wells in the SIII9 layer were optimized for well placement, leading to an incremental oil production of 2,526 tons (Table 4). These results demonstrate the effectiveness of the development adjustments.

By utilizing this technology, the spatial variation of sand bodies between wells was accurately identified, and the types of residual oil were clarified. This provided clear direction for the development adjustment strategies in the study area, optimizing the recovery of remaining oil and improving the overall production performance.

The three-dimensional attribute fusion technology based on lithology probability analysis provides a new approach for predicting single-phase river channels. It enables the quantitative selection of seismic attributes and better utilizes the advantages of different attributes. By adopting suitable seismic attribute fusion methods according to the geological conditions of different regions, this approach can more accurately describe subsurface geological features and reduce the uncertainties in seismic reservoir prediction caused by relying on a single attribute. This method plays a crucial role in improving the accuracy of sandbody boundary prediction and enhances the effectiveness of seismic data in complex geological environments.

Conclusions

Development of 3D Attribute Fusion Technology Based on Lithology Probability Analysis.

A novel 3D attribute fusion method based on lithology probability analysis has been developed. By optimizing and merging amplitude attributes that highlight the distribution of sedimentary sand bodies and coherence attributes that emphasize boundary variations, this method addresses the challenges of attribute selection and the low accuracy in river channel prediction typically associated with using a single attribute. This approach minimizes human intervention in seismic data processing, enabling accurate identification of river channels from a single seismic survey.

Three-dimensional seismic attributes fusion technology involves assigning a fixed value to the coherence attribute and integrating it into the amplitude volume to create a new fusion volume. This method alters certain boundary values within the fusion volume, strengthening weaker boundaries. It is particularly suitable for areas with weak coherence between connected sand bodies. By expanding the coherence range, this approach enhances the recognizability of sand body boundaries, making it especially effective for identifying continuous sand bodies in complex geological settings.

The filtering fusion method involves selecting two or more seismic attribute volumes, using one as the base and filtering out certain values from the other attributes. This method effectively retains the geological information captured in the seismic data, improving the accuracy of sand body connectivity identification. It is particularly useful in areas with significant coherence variation, where determining the connectivity between sand bodies is critical. In high-density well networks, this method is especially effective in identifying internal sand body boundaries.

The sedimentary facies maps generated through this technology guided the adjustment of 112 wells, leading to a total increase of 10,861 tons of oil, demonstrating the effectiveness of the method in optimizing reservoir development. This technique has proven to be highly effective and offers considerable potential for broader applications in reservoir characterization and development planning.

Data availability

The data supporting the research results can be obtained from China Petroleum & Natural Gas Corporation Daqing Oilfield, but the availability of these data is limited. These data are used under the permission of the current research, so they are not disclosed. However, the author can provide data according to reasonable requirements

and with the permission of China Petroleum & Natural Gas Corporation Daqing Oilfield. If anyone wants to obtain data from this study, please contact the corresponding author Zhang Shanyi.

Received: 2 December 2024; Accepted: 16 May 2025

Published online: 22 May 2025

References

- 1. Barakat, M., Azab, A. A. & Michael, N. Reservoir characterization using the seismic refection data: Bahariya formation as a case study Shushan basin North Western desert Egypt. *J. Petrol. Min. Eng.* https://doi.org/10.21608/jpme.2022.110315.1107 (2022).
- 2. Liu, Z. F. Review on oil and gas seismogeology models. J. Lithologic Reservoirs. 30 (1), 19–29 (2018).
- 3. Zeng, H. et al. Guidelines for seismic sedimentologic study in non-marine postrift basins. *J. Petroleum Explor. Dev.* **39** (3), 275–284 (2012).
- 4. Hong, Y. et al. Prediction of the favorable hydrocarbon accumulation zone in some oilfield in Liaohe by means of cluster analysis of seismic attributes. J. J. Xi' Shiyou Univ. 22 (4), 35–40 (2007).
- 5. Liu, X. Fine seismic processing and interpreting techniques for the thin and narrow sandbodies in lithologic oil reservoirs. *J. Petroleum Geol. Oilfield Dev. Daqing.* **36** (4), 137–141 (2017).
- 6. Noureldin, A. M., Mabrouk, W. M. & Metwally, A. M. Superimposed structure in the Southern periphery of Abu gharadig basin, Egypt: implication to petroleum system. *J. Contribut Geophys. Geodesy.* **53** (2), 97–110 (2023).
- Radwan, A. E. et al. Diagenetic overprint on porosity and permeability of a combined conventional unconventional reservoir: insights from the eocene pelagic limestones, Gulf of Suez Egypt. Mar. Petrol. Geol. 146, 105967. https://doi.org/10.1016/j.marpege o.2022.105967 (2022).
- 8. Dunham, R. J. in Classification of Carbonate Rocks According To Depositional Texture. 108–121 (eds Ham, W. E.) (Classification of Carbonate Rocks, AAPG, 1962).
- Shehata, A. A., Kassem, A. M., Brooks, H. L., Zuchuat, V. & Radwan, A. E. Facies analysis and sequence-stratigraphic control on reservoir architecture: example from mixed carbonate/siliciclastic sediments of Raha formation, Gulf of Suez, Egypt. *Mar. Petrol. Geol.* https://doi.org/10.1016/j.marpetgeo.2021.105160 (2021).
- 10. El-Nikhely, A. et al. Decoding of seismic data for complex stratigraphic traps revealing by seismic attributes analogy in Yidma/ Alamein concession area Western desert Egypt. *J. Petrol. Explor. Prod. Technol.* 12 (12), 3325–3338. https://doi.org/10.1007/s1320 2-022-01527-9 (2022).
- 11. Mohamed, H. S., Senosy, M. M. & Zaher, M. A. Corrigendum to interactive interpretation of airborne gravity, magnetic, and drill-hole data within the crustal framework of the Northern Western desert, Egypt. *J. Appl. Geophys.* **143**, 239. https://doi.org/10.1016/j.jappgeo.2016.12.007 (2017).
- 12. Adam, L., Batzle, M. & Brevik, I. Gassmann's fuid substitution and shear modulus variability in carbonates at laboratory seismic and ultrasonic frequencies. *J Geophysics* 71, F173–F183. https://doi.org/10.1190/1.2358494(2006).
- 13. El-Gendy, N. et al. Pre-Stack imaging for the Messinian sub salt sequences in the Levantine basin of the East mediterranean: a case study of shore Lebanon. *J. Iraqi Geol.* https://doi.org/10.46717/igj.56.1f.1ms-2023-6-9 (2023).
- 14. Dolson, J. C. et al. Te Petroleum Potential of Egypt. In: Downey, M.W., Treet, J.C. & Morgan, W.A. (eds) Petroleum Provinces of the Twenty-First Century. American Association of Petroleum Geologists Memoir. 74, 453–482. (6) (PDF) South Alamein petroleum system (Western Desert, Egypt). (2001).
- 15. Noureldin, A. M., Mabrouk, W. M. & Metwally, A. Delineating tidal channel feature using integrated post-stack seismic inversion and spectral decomposition applications of the upper cretaceous reservoir Abu Roash/C: a case study from Abu-Sennan oil feld Western desert Egypt. *J. Afr. Earth Sci.* https://doi.org/10.1016/j.jafrearsci.2023.104974 (2023).
- 16. Lin, C. Y. & Zhang, X. G. Development and prospect of petroleum seismogeology. J. Lithologic Reservoirs. 23 (1), 17-21 (2011).
- 17. Sarhan, M. A. Seismic Wireline logs sequence stratigraphic analyses and geologic evolution for the upper cretaceous succession of Abu gharadig basin Egypt. *J. Afr. Earth Sci.* 129, 469–480. https://doi.org/10.1016/j.jafrearsci.2017.02.004 (2017).
- 18. Noureldin, A. M., Mabrouk, W. M. & Metwally, A. Structural and petroleum system analysis using seismic data interpretation techniques to upper cretaceous rock units: a case study, West Abu-Sennan oil Feld, Northern Western desert Egypt. *J. Afr. Earth Sci.* 1 (198), 104772. https://doi.org/10.1016/j.jafrearsci.2022.104772 (2023).
- 19. Amer, M. et al. Tree-Dimensional integrated Geo-Static modeling for prospect identification and reserve Estimation in the middle miocene Multi-Reservoirs: A case study from Amal field Southern Gulf of Suez Province abstract. *J. Nat. Resour. Res.* 32 (6), 2609–2635. https://doi.org/10.1007/s11053-023-10253-w (2023).
- 20. Bosworth, W. & Tari, G. Hydrocarbon accumulation in basins with multiple phases of extension and inversion: examples from the Western desert (Egypt) and the Western black sea. J. Solid Earth. 12 (1), 59–77. https://doi.org/10.5194/se-12-59-2021 (2021).
- 21. Schlumberger Petrel E&P sofware (Version 2017) [Computer sofware]. (2017). Retrieved from https://www.sofware.slb.com/products/petrel
- 22. Ahmed, M. et al. Noureldin formation evaluation of Abu Madi reservoir in Baltim gas feld nile Delta using well logs core analysis and pressure data abstract. Sci. Rep. 13 (1). https://doi.org/10.1038/s41598-023-46039-6 (2023).
- 23. Barakat, M. & Nooh, A. Z. Reservoir quality using the routine core analysis data of Abu Roash C in Badr El Din-15 oil Feld, Abu gharadig basin, North Western desert Egypt. J. Afr. Earth Sci. 129, 683–691. https://doi.org/10.1016/j.jafrearsci.2017.02.019 (2017).
- 24. Yilmaz, O. & Taner, M. T. Discrete plane-wave decomposition by east-mean-square-error method. J. Geophys. 59 (6), 973–982 (1994).
- Pingsheng, W. E. I., Jianguo, P. A. N. & Huquan, Z. H. A. N. G. t al. Concepts method and technology of seismic reservoir. J. Lithologic Reservoirs. 22(2), 1–6 (2010).
- 26. Smith, T., Sondergeld, C. & Rai, C. Gassmann fuid substitutions: A tutorial. J. Geophys. 68, 430–440. https://doi.org/10.1190/1.156 7211 (2003).
- 27. GPC WORKSHOP. (2023). https://gpcnew.com/ws2023/workshop2023.html
- Barakat, M., El-Gendy, N. & Elbastawesy, M. A. Structural modeling of the Alam EL-Bueib formation in the Jade oil Feld, Western desert Egypt. J. Afr. Earth Sci. 156, 168–177. https://doi.org/10.1016/j.jafrearsci.2019.05.003 (2019).
- 29. Shapiro, S. A., Rothert, E., Rath, V. & Rindschwentner, J. Characterization of fuid transport properties of reservoirs using induced microseismicity. *J. Geophys.* 67, 212–220 (2002).
- 30. Li, D. G. & Liu, N. J. R. Reservoir prediction with integrated information based on artificial neural network technology and geostatistics. J. Oil&Gas Geol. 31 (4), 493–498 (2010).
- Sarhan, M. A. & Collier, R. E. L. Distinguishing rif-related from inversion-related anticlines: observations from the Abu gharadig and Gindi basins, Western desert Egypt. J. Afr. Earth Sci. 145, 234–245. https://doi.org/10.1016/j.jafrearsci.2018.06.004 (2018).
- 32. Fong, Y. L., Jiang, S. & Wang, C. F. Sequence stratigraphy, sedimentary systems and petroleum plays in a low-accommodation basin: middle to upper members of the lower jurassic Sangonghe formation, central Junggar basin, Northwestern China. *J. Asian Earth Sci.* 105, 85–103. https://doi.org/10.1016/j.jseaes.2015.03.025 (2015).
- 33. Noureldin, A. M., Mabrouk, W. M., Chikiban, B. & Metwally, A. Formation evaluation utilizing a new petrophysical automation tool and subsurface mapping of the upper cretaceous carbonate reservoirs, the Southern periphery of the Abu-Gharadig basin, Western desert, Egypt. J. Afr. Earth Sci. https://doi.org/10.1016/j.jafrearsci.2023.104977 (2023).

- 34. Sarhan, M. A. Geophysical assessment and hydrocarbon potential of the cenomanian Bahariya reservoir in the Abu gharadig field, Western desert Egypt. J. Petrol. Explor. Prod. Technol. 11 (11), 3963–3993. https://doi.org/10.1007/s13202-021-01289-w (2021).
- 35. Pijnenburg, R., Verberne, B., Hangx, S. & Spiers, C. Deformation behavior of sandstones from the seismogenic Groningen gas Feld: role of inelastic versus elastic mechanisms. *J. Geophys. Res. Solid Earth.* 123, 5532–5558 (2018).
- 36. Liu, A. Q. & Ren, C. D. Y. Frequency decomposition and waveform cluster analysis techniques Yinggehai basin gas field in the deep area of application. *J. Progress Geophys.* 28 (3), 338–344 (2018).
- 37. El-Ata, A. S. A. et al. Seismic characteristics and AVO response for non-uniform miocene reservoirs in ofshore Eastern mediterranean region Egypt. Sci. Rep. https://doi.org/10.1038/s41598-023-35718-z (2023).
- 38. Qi, H. et al. Application of seismic sedimentology in thin reservoir prediction: taking the identification of underwater fan in L87 well area as an example. *J. Progress Geophys.* **32** (2), 0709–0713 (2017).
- 39. Taner, M. T., Koehler, F. & Sherif, R. E. Complex seismic trace analysis. J. Geophys. 44 (6), 1041-1063 (1979).
- 40. Smith, J. A., Johnson, B. R. & Williams, C. D. Advances in visual porosity analysis: integrating microscopic and imaging approaches. *J. Petrol.* 45 (3), 567–582 (2021).
- 41. Zhang, J. Research and application of thin reservoir prediction techniques based on multiple linear regression in Shengli exploration area. *J. Chinese Journal of Engineering Geophysics*. 10(1), 91–94(2013). (2013).
- 42. Sarhan, M. A. & Selim, E. S. Geophysical appraisal of fractured carbonate reservoirs: a case study of Abu Roash D member, Abu gharadig field, Western desert, Egypt. Euro-Mediterranean. *J. Environ. Integr.* 8 (2), 395–408. https://doi.org/10.1007/s41207-023-00365-3 (2023).
- 43. Jia, H. B. et al. A retreating fan-delta system in the Northwestern Junggar basin, Northwestern China-Characteristics, evolution and controlling factors. J. Asian Earth Sci. 123, 162–177. https://doi.org/10.1016/j.jseaes.2016.04.004 (2016).
- 44. Tingting, L. I., Zhao, W. A. N. G. & Shizhong, M. A. el al. Summary of seismic attributes fusion method. J. Progress in Geophysics. 378–385. (2015)(1).
- 45. Zhao, D. N., Zhu, X. M., Dong, Y. L., Wu, D. & Zhu, M. Application of seismic sedimentology to prediction of beach and bar sandbodies in gentle slope of lacustrine basin: A case study of the lower cretaceous in chepaizi area, Junggar basin, NW China. *Pet. Explor. Dev.* 41 (1), 60–67. https://doi.org/10.1016/S1876-3804(14)60006-9 (2014).

Author contributions

Shanyi Zhang is responsible for the main technical aspects of the entire paper, while the other authors (Xueying Li, Jinyu Lan, Dejian Zhang, Lin Cong, Yaning Shi) are responsible for the application. All authors have reviewed the manuscript.

Declarations

Competing interests

The authors declare no competing interests.

Additional information

Correspondence and requests for materials should be addressed to S.Z.

Reprints and permissions information is available at www.nature.com/reprints.

Publisher's note Springer Nature remains neutral with regard to jurisdictional claims in published maps and institutional affiliations.

Open Access This article is licensed under a Creative Commons Attribution-NonCommercial-NoDerivatives 4.0 International License, which permits any non-commercial use, sharing, distribution and reproduction in any medium or format, as long as you give appropriate credit to the original author(s) and the source, provide a link to the Creative Commons licence, and indicate if you modified the licensed material. You do not have permission under this licence to share adapted material derived from this article or parts of it. The images or other third party material in this article are included in the article's Creative Commons licence, unless indicated otherwise in a credit line to the material. If material is not included in the article's Creative Commons licence and your intended use is not permitted by statutory regulation or exceeds the permitted use, you will need to obtain permission directly from the copyright holder. To view a copy of this licence, visit https://creativecommons.org/licenses/by-nc-nd/4.0/.

© The Author(s) 2025